

# How Strain Affects the Reactivity of Surface Metal Oxide Catalysts

Kazuhiko Amakawa, Lili Sun, Chunsheng Guo, Michael Hävecker, Pierre Kube, Israel E. Wachs, Soe Lwin, Anatoly I. Frenkel, Anitha Patlolla, Klaus Hermann, Robert Schlögl and Annette Trunschke\*

In 1925, Sir H.S. Taylor proposed that special active sites in a non-balanced state (*e.g.* low-coordinated species), which represent only a fraction of the surface atoms, are responsible for heterogeneous catalysis.<sup>[1]</sup> It took decades until the concept earned experimental and theoretical confirmation. Surface science proved that low-coordinated atoms at the edge of steps are indeed the most active in metal catalysts.<sup>[2]</sup> Recent advances in materials characterization revealed that Sir Taylor's concept is also applicable to high-performing, multi-component catalysts, *e.g.* nanostructured Cu/ZnO for methanol synthesis<sup>[3]</sup> and supported gold nanoparticles<sup>[4]</sup>, wherein ensemble sites formed at surface defects or at the metal-oxide interface play a crucial role for catalytic behavior.

Monolayer-type supported metal oxides represent another important class of heterogeneous catalysts, in which the supported metal oxide phase is present as a two-dimensional surface overlayer,

that also seem to be characterized by differences in the reactivity of the individual surface metal oxide species. Recalling Sir Taylor's concept, only ~1.5% of the molybdenum atoms are active in olefin metathesis over silica supported molybdenum oxide catalysts.<sup>[5]</sup> The catalytic performance of supported metal oxides sometimes shows a non-linear dependence on the metal oxide loading where the activity develops steeply above a certain level of surface coverage.<sup>[6–10]</sup> Reasons for this general observation, however, remain elusive.

In the present work, silica-supported molybdena, which represents a model for oxidation<sup>[8]</sup> and metathesis<sup>[5,9]</sup> catalysts, was chosen to exemplify the impact of surface metal oxide coverage on reactivity. Dehydrated<sup>[11]</sup> molybdenum oxide supported on mesoporous silica SBA-15 (MoO<sub>x</sub>/SBA-15) was initially studied by temperature-programmed reduction with hydrogen (H<sub>2</sub>-TPR) as a test reaction.<sup>[6,9,10]</sup> The H<sub>2</sub>-TPR profiles (Figure 1) reveal enhanced reducibility with increasing Mo oxide loading. At the lowest loading (2.1% Mo), a single, sharp reduction peak is observed at 1158 K. Upon increasing the Mo oxide loading, a new distinct low temperature peak at 856 K occurs in addition to the progressive broadening of the high temperature peak, indicating cumulative appearance of surface molybdena species exhibiting higher reducibility.

[\*] Dr. K. Amakawa, Dr. L. Sun, Dr. C. S. Guo, Dr. M. Hävecker, P. Kube, Prof. Dr. K. Hermann, Prof. Dr. R. Schlögl, Dr. A. Trunschke  
Department of Inorganic Chemistry  
Fritz-Haber-Institut der Max Planck Gesellschaft  
Faradayweg 4-6, 14195 Berlin (Germany)  
E-mail: [trunschke@fhi-berlin.mpg.de](mailto:trunschke@fhi-berlin.mpg.de)  
Homepage: <http://www.fhi-berlin.mpg.de/>

Dr. M. Hävecker  
Department of Solar Energy Research  
Helmholtz-Zentrum Berlin/BESSY II  
Albert-Einstein-Str. 15, 12489 Berlin (Germany)

Prof. Dr. I. E. Wachs, S. Lwin  
Operando Molecular Spectroscopy & Catalysis Laboratory  
Department of Chemical Engineering  
Lehigh University  
Bethlehem, Pennsylvania 18015 (USA)

Prof. Dr. A. I. Frenkel, Dr. A. Patlolla  
Department of Physics  
Yeshiva University  
245 Lexington Avenue, New York, NY 10016 (USA)

[\*\*] We thank G. Weinberg, Dr. T. Cotter, M. Hashagen, G. Lorenz, Dr. F. Girgsdies, E. Kitzelmann, A. Klein-Hoffmann, C.V.T. Nguyen, the NSLS staff, and the HZB staff for their professional assistance. Prof. Dr. I.E. Wachs thanks the Alexander von Humboldt Foundation, Germany, for the Humboldt Research Award. Prof. Dr. A. I. Frenkel acknowledges the U.S. DOE Grant No. DE-FG02-05ER15688 for supporting X18B beamline operations. S. Lwin and C.V.T. Nguyen acknowledge financial support from U.S. DOE-Basic Energy Sciences (Grant No. FG02-93ER14350) and NSF-Research Experience for Undergraduates (Grant No. CBET-1134012), respectively. K. Amakawa is grateful to Mitsubishi Gas Chemical Co. Inc. for a fellowship.

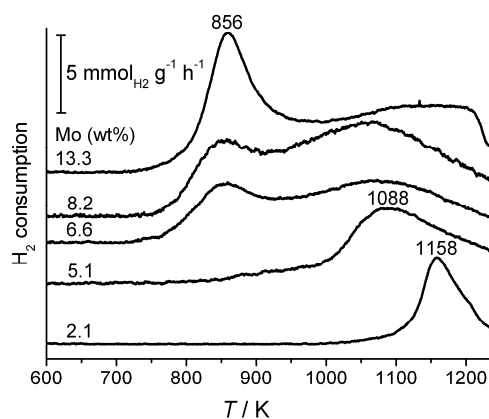


**Figure 1.** Temperature-programmed reduction (H<sub>2</sub>-TPR) of supported MoO<sub>x</sub>/SBA-15 measured at a heating rate of 10 K min<sup>-1</sup> in 2% H<sub>2</sub> in Ar after pretreatment in 20% O<sub>2</sub> in Ar at 823 K for 0.5 h.

The effect of surface coverage on the reactivity of monolayer transition metal oxides has been attributed to changes in the degree of polymerization *e.g.*, the appearance of monomeric, polymeric and nano-crystalline domains.<sup>[7]</sup> In the present case, however, spectroscopy reveals only modest structural modifications with increasing surface coverage. The very similar fingerprints in the Mo K-edge x-ray absorption near edge structure (XANES) and UV-vis spectroscopy (Figure 2 a and b) indicate little change in the

connectivity of surface molybdena<sup>[12]</sup> and in the coordination geometry, featuring a predominantly tetrahedral coordination similar to the reference  $\text{Al}_2(\text{MoO}_4)_3$  as suggested by the intense pre-edge peak at 20006 eV (Figure 2b). Fourier-transformed Mo K-edge extended x-ray absorption fine structure (EXAFS) spectra (Figure 2c) show two distinct distances at  $R < 2\text{Å}$ , which are assigned to Mo=O double and Mo—O single bonds referring to the observed vibrational bands in the Raman/IR analysis<sup>[13–16]</sup> (Supporting Information; Figure S6, 980–997  $\text{cm}^{-1}$  for Mo=O, and 926–943  $\text{cm}^{-1}$  for Mo—O). Conclusive structural assignment is provided by near edge x-ray absorption fine structure (NEXAFS) analysis at the O K-edge combined with DFT calculations. The double-peak absorption at the O 1s edge (Figure 2d; peaks at 530.2 and 532.5 eV) observed at low loadings is well reproduced by DFT calculations<sup>[17]</sup> considering models having two-fold anchored di-oxo ( $\text{Si—O—})_2\text{Mo(=O)}_2$  structures characterized by a Si—Si distance of 4.6–4.7 Å (Supporting Information; clusters **a** and **b** in Figure S1, Figure S5A, Table S1). In accordance with this result, the fitting of the first coordination sphere of Mo in the K-edge EXAFS using a di-oxo ( $\text{O—})_2\text{Mo(=O)}_2$  model reproduces the experimental spectra well, yielding Mo—O path lengths consistent with the theoretical prediction (Supporting Information; Figures S1, S4, Tables S1, S3). Moreover, the calculated IR spectra of the di-oxo models are in agreement with the experimental IR spectra (Supporting Information; Figures S6D, S7). All the results indicate that the two-fold anchored tetrahedral di-oxo ( $\text{Si—O—})_2\text{Mo(=O)}_2$  unit represents the major surface molybdena species, which is also in agreement with previous reports.<sup>[13–17]</sup>

While the bond lengths obtained by EXAFS fitting are independent of the Mo loading (Supporting Information; Table S3), subtle structural variations are clearly imprinted in the O K-edge NEXAFS data. The O K-edge NEXAFS feature due to molybdena (528–534 eV) gradually loses the well-separated double peak structure by broadening of the peaks and occurrence of a new component at 531 eV (Figure 2d). The peak broadening and the occurrence of the new peak seem to be linked to the changes in the  $\text{H}_2$ -TPR profiles (Figure 1; broadening of the high temperature peak and the occurrence of the low temperature peak at 856 K). The broad NEXAFS feature is in clear contrast to the well separated double peak corresponding to crystalline  $\text{Na}_2\text{MoO}_4$  (Figure 2d) that consists of uniform isolated  $\text{MoO}_4$  units, implying changes in the bond angles due to variations in the Mo—Si distance with increasing loading. The Fourier transform of the Mo K-edge EXAFS at longer  $R$  (Figure 2c) shows neither distinct peaks nor systematic changes upon increasing the Mo loading, which indicates the absence of a well-defined geometrical order beyond the first coordination sphere and suggests, in turn, a broad distribution of the Mo—Si distance of anchoring Mo—O—Si motifs. The various Mo—Si distances originate from the amorphous nature of the silica surface that provides a distribution in the Si—Si distance of silanol pairs used for anchoring of the di-oxo structures.<sup>[13,18,19]</sup> This leads to variations in the Mo—O—Si angle and O—Si length. In addition, four-fold coordinated pentahedral mono-oxo ( $\text{Si—O—})_4\text{Mo=O}$  structures may occur as a minority when four silanol sites are suitably arranged.<sup>[13]</sup> In fact, we observe additional vibrational bands assigned to the mono-oxo species<sup>[13,14]</sup> in the resonance Raman analysis that detects minority species that are invisible in non-resonant Raman (Supporting Information; Figure S8).

Surface silanol groups are consumed by forming Mo—O—Si bridging bonds. The density of isolated silanol sites drops from 1.6 (bare SBA-15) to 0.07 (13.3% Mo) sites per square nanometer (Supporting Information; Table S2, Figure S6C), revealing a highly

“silanol deficient” state at high Mo oxide surface coverage. Given the limited availability of silanol groups at high coverage, the formation of surface molybdena species having plural anchoring bonds (e.g. two-fold anchored di-oxo structure) involves the impact of strain. The models in Figure 3 illustrate the idea schematically. The two-dimensional ( $x$ – $y$  axes) description in Figure 3a shows a network of siloxane rings comprising various ring sizes,<sup>[18,20]</sup> while another two dimensional description in Figure 3b reminds us that there is also a variation in the third axis  $z$  in real 3D space. In Figure 3a, the di-oxo  $\text{MoO}_4$  units are anchored on less strained configurations at low molybdenum coverage, whereas the decrease of silanol sites forces the di-oxo  $\text{MoO}_4$  structures to form more strained configurations. The distribution of species is most likely governed by the thermodynamic stability<sup>[21]</sup> due to the high surface mobility of molybdena.<sup>[11,22]</sup> In the 2D description, the geometric constraint may be approximated by the size of the smallest molybdosiloxane ring that belongs to the di-oxo  $\text{MoO}_4$  unit as illustrated in Figure 3a. Extending the 2D model into the real 3D space further increases the variation of combinations of available silanol sites (even within the same size of a molybdosiloxane ring).

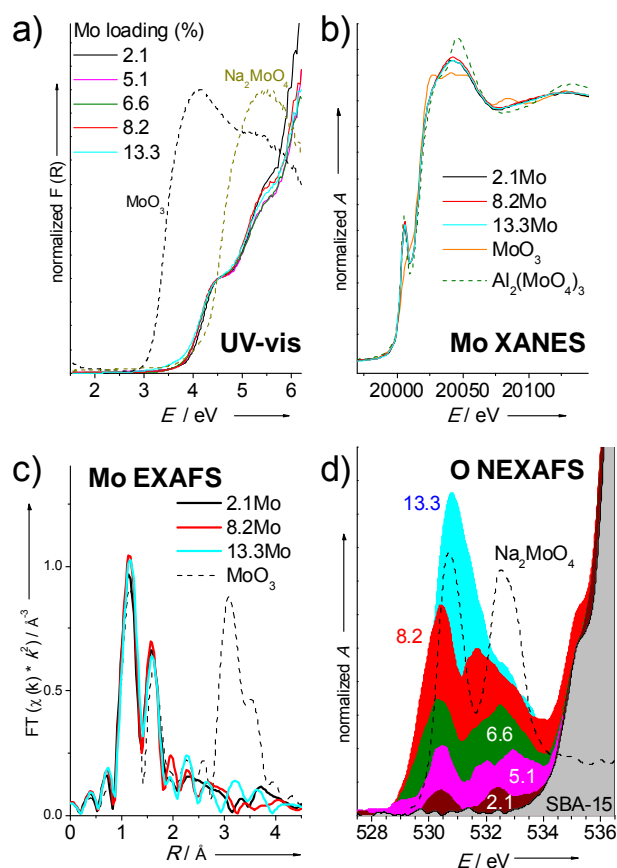
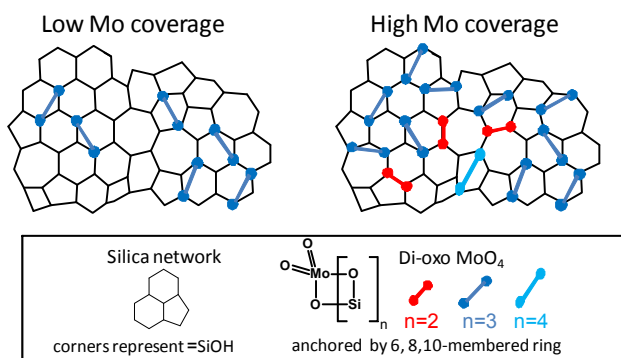


**Figure 2.** (a) UV-vis, (b) Mo K-edge XANES, (c) Fourier-transformed phase-uncorrected Mo K-edge EXAFS, and (d) O K-edge NEXAFS spectra of dehydrated  $\text{MoO}_x/\text{SBA-15}$ .

Strain at the anchoring bonds leads also to a high potential energy at the location, which very likely enhances the reactivity considering the Brønsted–Evans–Polanyi relation,<sup>[23,24]</sup> which seems also applicable to metal oxides.<sup>[25]</sup> Accordingly, the increased reducibility at high Mo oxide coverage (Figure 1) is explained by the increased strain of surface molybdena species predominantly

consisting of di-oxo MoO<sub>4</sub> structures. The occurrence of a distinct low temperature peak at 856 K in the H<sub>2</sub>-TPR profile may reflect the presence of a discrete Si—Si distance (which may be related to a specific molybdosiloxane ring size) that accommodates a surface molybdena species, which is particularly reactive towards hydrogen. This is plausible because the flexibility of the siloxane network is not infinite.

### a) top view



### b) side view

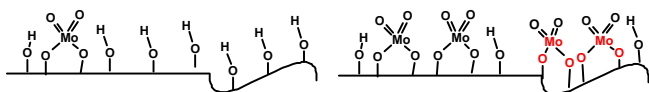


**Figure 3.** Schematic illustration of the suggested anchoring patterns of di-oxo ( $-\text{Si}-\text{O}-$ )<sub>2</sub>Mo(=O)<sub>2</sub> structures on a 2D silica surface at different surface molybdenum densities. Two 2D models (a, b) are shown to illustrate the real 3D space. The differently colored dots-terminated lines in “a” top view” represent the di-oxo species having different anchoring geometries.

As the availability of the anchoring surface hydroxyl sites is closely related to the impact of the strain, tuning the silanol population by thermal treatments (i.e. variation in the dehydration temperature) instead of changing the metal loading would also allow controlling of the frustration, leading to the change in the reactivity. In fact, the activity of silica-supported chromia catalysts used in ethylene polymerization (known as industrial Phillips catalysts) goes up with increasing the activation temperature up to 1198 K where progressive dehydroxylation takes places,<sup>[26–28]</sup> which may be rationalized in terms of the increased strain of the surface chromate species.<sup>[27–30]</sup>

To investigate the influence of the anchoring geometry on the O K-edge NEXAFS feature, we modeled a highly strained di-oxo ( $-\text{Si}-\text{O}-$ )<sub>2</sub>Mo(=O)<sub>2</sub> structure (Supporting Information; cluster **c** in Figure S1) anchored on a silanol pair exhibiting a Si—Si distance of 3.07 Å, which is much shorter than that of other cluster models (4.6–4.7 Å) (Supporting Information; Figure S1, Table S1). The geometric constraint results in significant modification of the O=Mo=O angle and the Mo=O bond lengths, which drastically affects the NEXAFS feature (Supporting Information; Table S1, Figure S5A). Modification of the cluster model by changing the O=Mo=O bond angle while freezing other geometric parameters results in a strong systematic change in the calculated O K-edge NEXAFS spectra (data not shown). It was found that some of the angle-modified di-oxo clusters show intense absorption at 531 eV

(Supporting Information; Figure S5B), which may account for the increased absorption at around 531 eV observed in the experimental spectra of the high-coverage samples (Figure 2d). As MoO<sub>x</sub>/SBA-15 has a distribution of species as evidenced by H<sub>2</sub>-TPR, the observed O K-edge NEXAFS spectra are a convoluted integral of all the species present, which cannot be readily simulated by the limited number of model clusters considered here. Nevertheless, these theoretical observations suggest that an increased distortion of the tetrahedral geometry of the ( $-\text{Si}-\text{O}-$ )<sub>2</sub>Mo(=O)<sub>2</sub> units due to limitations in space on the silica surface may be the reason for the observed changes in the O K-edge NEXAFS spectra. The stronger structure sensitivity of the O K-edge NEXAFS versus UV-vis and Mo K-edge XANES may be related to the fact that the O K-edge NEXAFS probes the excitation of electrons in the isotropic (i.e. spherical) O 1s core orbitals of all the O atoms coordinated to the Mo center into the unoccupied Mo 4d—O 2p orbitals that are anisotropic.

In addition to the strain imposed by the Mo—O—Si anchoring bonds, lateral interactions between vicinal surface molybdena species come into play at higher coverage, which can influence spectroscopic features and reactivity as well. The DFT calculations clearly reveal a repulsive interaction of two adjacent tetrahedral di-oxo MoO<sub>4</sub> units (Supporting Information; cluster **b** in Figure S1). Increasing the surface density of MoO<sub>x</sub> species may induce O—O interactions, resulting in a modification of the O=Mo=O angle or other geometric parameters. Likewise, structural perturbations due to the hydrogen bonding between surface silanol groups and surface molybdena species may also influence the reactivity. In fact, the occurrence of hydrogen bonding is clearly visible in the IR/Raman spectra where the stretching vibrations due to hydroxyl and molybdenum—oxygen exhibit a red shift when Si-OH and surface molybdena coexist (Supporting Information; Figure S6B,C).

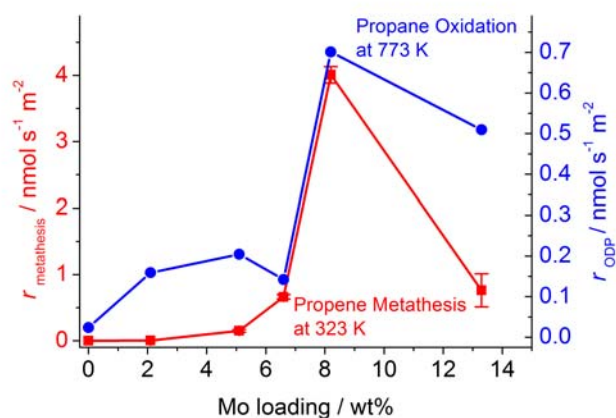


**Figure 4.** Specific rates of product formation for propene metathesis at 323 K, and oxidative dehydrogenation of propane (ODP) at 773 K over MoO<sub>x</sub>/SBA-15. Selectivity to desired product(s) was > 99.5% and 49–83% for propene metathesis and ODP, respectively. Selectivity data for ODP are presented in Figure S9 in the Supporting Information.

The H<sub>2</sub>-TPR (Figure 1) probes the distribution of surface molybdena species and provides information on all the molybdena species present. Following Sir Taylor’s concept, it is expected that only fractional “high energy sites” are reactive enough to perform catalytic turnovers at given conditions in heterogeneously catalyzed reactions. Indeed, a steep increase of catalytic activity at 8.2% of Mo loading was observed in both propene metathesis and oxidative

dehydrogenation of propane (Figure 4), manifesting the significant impact of the frustration of surface metal oxide species. The detailed dependencies differ due to the very different nature of the stoichiometric or catalytic reactions, the different reactants that have to be activated (H<sub>2</sub>, propene, propane and O<sub>2</sub>) and, consequently, the different demands on the corresponding active sites (Figures 1, 4, S9). The most complex reaction within the series studied is the oxidative dehydrogenation of propane due to the underlying complex network of consecutive and parallel reactions that determine the selectivity (Fig. S9). But also here the emerging frustration of surface metal oxide species with increasing loading is reflected in the formation rate of the product, since the activation of the methylene C-H bond in propane on surface metal oxide species has been proven to be the rate determining step.<sup>[33]</sup>

In summary, the remarkable increase of the reactivity of silica supported molybdena species at high Mo oxide surface coverage is related to an increased frustration of the surface molybdena species, which originates from geometric constraints of the anchoring bonds and additional lateral interactions of surface species. Given the similarity in the molecular structures of supported metal oxides,<sup>[14]</sup> the same scenario is likely to occur in monolayer-type supported metal oxides in general, especially for SiO<sub>2</sub> supports that tend to form isolated surface metal oxide sites.<sup>[14]</sup> Variation in the support material (e.g. alumina, titania, zirconia etc.) changes the nature of supported metal oxide species with respect to both the distribution of suitable geometric arrangements<sup>[31]</sup> and the electronic property.<sup>[32]</sup> Even given the complexity, strain-induced “high energy sites,” would locally occur at the metal-oxide—support interface whenever a distribution of the suitability of the anchoring sites exists, which is likely always the case.

We propose the frustration of the surface metal oxide species as an important and novel descriptor for catalysis over supported metal oxides to complement other structural classifications that have been considered (e.g. degree of polymerization, coordination patterns, etc.). Based on these insights, we argue that theoretical and experimental efforts in heterogeneous catalysis should focus more on metastable configurations that are usually less acknowledged due to their instability or minority status. Furthermore, applying the mechanistic concept of the formation of “high energy sites” presented here, a rational catalyst design would be feasible by choosing strategies that artificially increase the probability of the formation of “high energy sites.” For example, the use of promoter elements or tuning the surface structure of the support by physicochemical treatments (e.g. activation temperature as in the case of Phillips catalysts).

## Experimental Section

The MoO<sub>3</sub>/SBA-15 catalysts (Mo loading of 2.1~13.3 wt% / 0.2~2.5 Mo\_atoms nm<sup>-2</sup>) were prepared by an ion-exchange approach. Details regarding synthesis, characterization, DFT calculations, and catalytic test reactions are summarized in the Supporting Information.

Received:

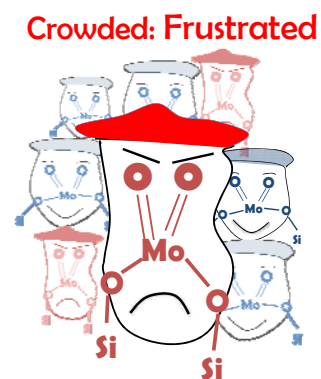
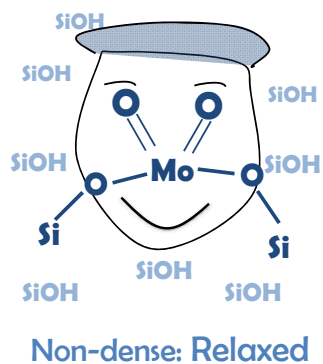
Published:

**Keywords:** heterogeneous catalysis · molybdenum · olefin metathesis · selective oxidation · supported catalysts

- [1] H. S. Taylor, *Proc. R. Soc. Lond. A* **1925**, *108*, 105–111.
- [2] T. Zambelli, J. Winterlin, J. Trost, G. Ertl, *Science* **1996**, *273*, 1688–1690.
- [3] M. Behrens et al., *Science* **2012**, *336*, 893–897.
- [4] I. X. Green, W. Tang, M. Neurock, J. T. Yates, *Science* **2011**, *333*, 736–739.
- [5] K. Amakawa, S. Wrabetz, J. Kröhnert, G. Tzolova-Müller, R. Schlögl, A. Trunschke, *J. Am. Chem. Soc.* **2012**, *134*, 11462–11473.
- [6] K. Chen, A. T. Bell, E. Iglesia, *J. Catal.* **2002**, *209*, 35–42.
- [7] I. E. Wachs, *Catal. Today* **2005**, *100*, 79–94.
- [8] T.-C. Liu, M. Forissier, G. Coudurier, J. C. Védrine, *J. Chem. Soc., Faraday Trans. 1* **1989**, *85*, 1607–1618.
- [9] R. Thomas, J. A. Moulijn, *J. Mol. Catal.* **1982**, *15*, 157–172.
- [10] Y. Lou, H. Wang, Q. Zhang, Y. Wang, *J. Catal.* **2007**, *247*, 245–255.
- [11] M. Boer, A. J. Dillen, D. C. Koningsberger, J. W. Geus, M. A. Vuurman, I. E. Wachs, *Catal. Lett.* **1991**, *11*, 227–239.
- [12] R. S. Weber, *J. Catal.* **1995**, *151*, 470–474.
- [13] J. Handzlik, J. Ogonowski, *J. Phys. Chem. C* **2012**, *116*, 5571–5584.
- [14] E. L. Lee, I. E. Wachs, *J. Phys. Chem. C* **2007**, *111*, 14410–14425.
- [15] S. Chempath, Y. Zhang, A. T. Bell, *J. Phys. Chem. C* **2007**, *111*, 1291–1298.
- [16] L. J. Gregoriades, J. Döbler, J. Sauer, *J. Phys. Chem. C* **2010**, *114*, 2967–2979.
- [17] C. S. Guo, K. Hermann, M. Hävecker, J. P. Thieleman, P. Kube, L. J. Gregoriades, A. Trunschke, J. Sauer, R. Schlögl, *J. Phys. Chem. C* **2011**, *115*, 15449–15458.
- [18] L. Lichtenstein, C. Büchner, B. Yang, S. Shaikhutdinov, M. Heyde, M. Sierka, R. Włodarczyk, J. Sauer, H.-J. Freund, *Angew. Chem. Int. Ed.* **2012**, *51*, 404–407.
- [19] S. Bordiga, S. Bertarione, A. Damin, C. Prestipino, G. Spoto, C. Lamberti, A. Zecchina, *J. Mol. Catal. A: Chem.* **2003**, *204–205*, 527–534.
- [20] F. Tielens, C. Gervais, J. F. Lambert, F. Mauri, D. Costa, *Chem. Mater.* **2008**, *20*, 3336–3344.
- [21] M. A. Banares, H. C. Hu, I. E. Wachs, *J. Catal.* **1994**, *150*, 407–420.
- [22] S. Braun, L. G. Appel, V. L. Camorim, M. Schmal, *J. Phys. Chem. B* **2000**, *104*, 6584–6590.
- [23] J. N. Bronsted, *Chem. Rev.* **1928**, *5*, 231–338.
- [24] M. G. Evans, M. Polanyi, *Trans. Faraday Soc.* **1938**, *34*, 11–24.
- [25] A. Vojvodic et al., *J. Chem. Phys.* **2011**, *134*, 244509–244509–8.
- [26] B. M. Weckhuysen, I. E. Wachs, R. A. Schoonheydt, *Chem. Rev.* **1996**, *96*, 3327–3350.
- [27] M. P. McDaniel, M. B. Welch, *J. Catal.* **1983**, *82*, 98–109.
- [28] M. P. McDaniel, in *Handbook of Heterogeneous Catalysis*, Wiley-VCH Verlag GmbH & Co. KGaA, **2008**.
- [29] E. Groppo, C. Lamberti, S. Bordiga, G. Spoto, A. Zecchina, *Chem. Rev.* **2005**, *105*, 115–184.
- [30] C. A. Demmelmaier, R. E. White, J. A. van Bokhoven, S. L. Scott, *J. Catal.* **2009**, *262*, 44–56.
- [31] G. Tsilomelekis, S. Boghosian, *Catal. Sci. Technol.* **2013**, DOI 10.1039/C3CY00057E.
- [32] T. Fievez, P. Geerlings, B. M. Weckhuysen, F. De Proft, *ChemPhysChem* **2011**, *12*, 3281–3290.
- [33] X. Rozanska, R. Fortrie, J. Sauer, *J. Phys. Chem. C* **2007**, *111*, 6041–6050.

## Heterogeneous Catalysis

K. Amakawa, L. Sun, C. S. Guo,  
M. Hävecker, P. Kube, I. E. Wachs, S.  
Lwin, A. I. Frenkel, A. Patlolla,  
K. Hermann, R. Schlögl, A. Trunschke\*  
\_\_\_\_\_ Page – Page



**Only uncomfortable seats left:** At high coverage where available anchoring surface hydroxyl sites are limited, surface metal oxide molecules are forced to be anchored in frustrated configurations, leading to an increased reactivity. The concept explains the sometimes observed non-linear coverage dependence in monolayer-type supported metal oxide catalysts.